Thermo-mechanical phenomena in the process of friction welding of corundum ceramics and aluminium

Z. LINDEMANN, K. SKALSKI, W. WŁOSIŃSKI, and J. ZIMMERMAN*

Institute of Mechanics and Design, Warsaw University of Technology, 85 Narbutta St., 02-524 Warszawa, Poland

Abstract. In the paper the modelling of thermo-mechanical effects in the process of friction welding of corundum ceramics and aluminium is presented. The modelling is performed by means of finite element method. The corundum ceramics contains 97% of Al_2O_3. The mechanical and temperature fields are considered as coupled fields. Simulation of loading of the elements bonded with the heat flux from friction heat on the contact surface is also shown. The heat flux was modified in the consecutive time increments of numerical solutions by changeable pressure on contact surface. Time depending temperature distribution in the bonded elements is also determined. The temperature distribution on the periphery of the cylindrical surfaces of the ceramics and Al was compared to the temperature measurements done with a thermovision camera. The results of the simulation were compared to those obtained from the tests performed by means of a friction welding machine.

Key words: friction welding, ceramics-metal bonding, finite element method, thermo-mechanical modelling, temperature field, displacement field.

1. Introduction

Bonding of metal and ceramic materials by means of friction welding is possible and successfully performed [1–4].

The analysed in the paper technological process of friction welding is applied to the end faces of two cylindrical elements made of corundum ceramics Al_2O_3 and aluminium alloy.

Knowledge of temperature distribution in the vicinity of the welded bond is significant in assessment of physical processes in the area of welding. The temperature gradient and plastic thermal deformations determine microstructural changes, diffusion phenomena and mechanical properties of the finished product. Unfavourable thermal and stress effects are intensified when materials of different heat and mechanical properties, like Al_2O_3 and Al, are bonded.

There are publications in which calculations of temperature distribution in the welding area are presented. In the earlier papers published in the 60 s – 80 s [5–8] one can find analytical calculations by means of which rough estimation of temperature distribution is possible. In the later publications calculations based on numerical solutions, i.e. finite difference method [9,10] and finite element method [11–15], are presented. In the paper [9] the authors assess the temperature values in the welding area on the basis of microstructure analysis of the weld. They also present a statistical analysis of the influence of welding parameters on the strength of copper-steel bonding. Ambroziak [10] determines the temperature fields in welding of infusible metals in liquid. He also present the results of temperature measurements performed by means of thermocouple. The authors of the above mentioned papers solve the problem as axisymmetric one assuming constant coefficient of friction and constant linear pressure distribution on the contact surface. The axial temperature distribution has

been studied by the authors of [15] in an analytical, numerical and experimental manner. Sluzalec [14] modelled the process friction welding of steel rods assuming contact on the friction surfaces and dependence of the coefficient of friction on temperature. He used thermoplastic material model and presented a theoretical model of coupled thermo-mechanical fields. He compared the calculated temperature distribution to that obtained from experiments. The authors [13] presented calculations of temperature distribution in the process of welding of metal rods of different diameters. Fu and Duan [12] determined temperature field and stress and strain fields in welded elements treating the problem as a coupled one. The other authors [11] showed finite element mesh deformed in the process of welding of metallic materials that differed in properties and compared the dimensions of welded elements to those obtained after experimental test. They applied visco-plastic material model and they took into account the influence of rheological and tribological parameters that were coupled to the mechanical load. All the papers mentioned above concern welding of metal elements and in the calculation the pressure distribution on the contact surface is assumed constant and linear. There are no publications on thermo-mechanical phenomena in the process of friction welding of ceramics and metal.

The aim of the researches described in the paper is to simulate the process of friction welding of cylindrical workpieces made of ceramics and aluminium alloy by means of finite element method with special consideration for temperature and deformation distributions. Knowledge of those distributions as well as their changes with time are very helpful in explaining the phenomena that take place during the process. The way of loading of the bonded elements with heat flux, which is modified in the consecutive time increments of the numerical solution, is an innovative aspect of the qualitative assessment of

---

*e-mail: jolz@wip.pw.edu.pl

the process. On the basis of such performed numerical calculations one can make valuable conclusions on the quality of the weld.

2. Physical model of the process

In the friction welding test cylindrical workpieces of 10 mm diameter made of aluminium and corundum ceramics (97% Al_2O_3) were used. The diagram of the process is shown in Fig. 1. The friction welding process consisted of the following steps:

1. Friction heating under pressure of 18 MPa (the ceramic workpiece is given a rotational velocity 14500 r.p.m., it rubs the end face of the aluminium workpiece fixed in the vice). In this stage any surface irregularities are removed, the temperature is increasing, in the vicinity of the welded surfaces an interface of visco-plastic aluminium is being formed.

2. The forging stage consists with: stopping rotation of the ceramic workpiece, increasing the pressure to 46 MPa. There are significant thermo-plastic deformation of aluminium in the contact area. In result of this is formation of a flange-like flash. The process of welding takes place due to the plastic and diffusion effects.

3. The stage of cooling down to the moment of temperature equalisation between the workpieces and the environment.

In Fig. 2 the experimental run of loading with time is shown. The run of rotational velocity of the ceramic workpiece is denoted with the thin line.
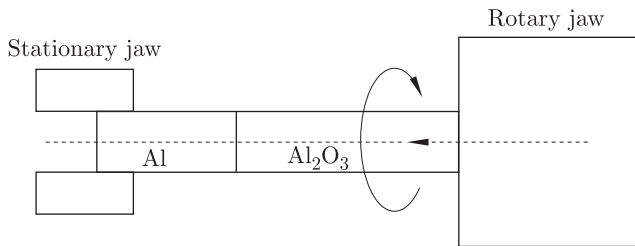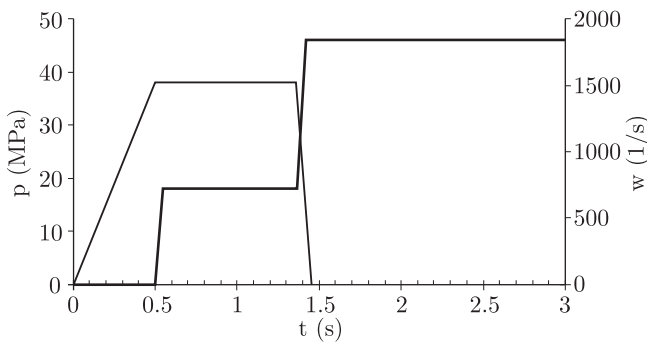

Fig. 1. Diagram of friction welding process

Fig. 2. Load change with time

3. Mathematical modelling of temperature distribution

In order to determine temperature distribution we started from equation of heat transfer, which, assuming no internal heat source, can be written for homogenous isotropic materials of ceramics and metal (V^C, V^M) in the index notation as follows [16]:

$$(k_i T_{,i})_{,i} = T_{,t}$$
$$i = x, y, z \text{ (no sum on i in parentheses)} \tag{1}$$

where: $k = k_x = k_y = k_z$, $k = \frac{\lambda}{c_p \rho} \left[\frac{m^2}{s}\right]$ – coefficient of thermal conductance, $\rho \left[\frac{kg}{m^3}\right]$ – material density, $\lambda \left[\frac{J}{smK}\right]$ – thermal conductivity, $c_p \left[\frac{J}{kgK}\right]$ – specific heat.

The differential Eq. (1) has the unique solution when proper boundary conditions are formulated. In the modelled process (Fig. 3) it is assumed that there is no heat exchange between the end faces S^C, S^M and environment (flux $q^C = q^M = 0$) and that temperature distribution on those faces is known.

$$T|_{S^C} = T^0; \quad T|_{S^M} = T^0. \tag{2}$$

It is also assumed that intensity of heat flux on the material boundary (S^K) is known and can be calculated by means of the known Fourier equation:

$$-\lambda_n^C T_{,n} = q^C, \quad -\lambda_n^M T_{,n} = q^M, \quad q^{S^K} = q^C + q^M \tag{3}$$

n – normal direction, $\lambda_n = \lambda_x = \lambda_y = \lambda_z = \lambda$ for isotropic materials.
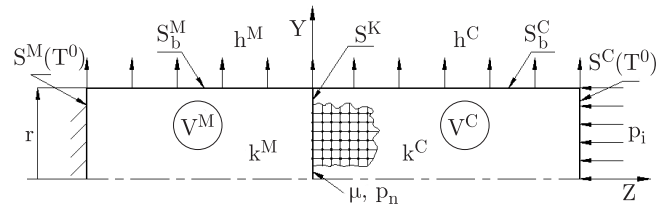

Fig. 3. Modelling of friction welding

The heat flux q^{S^K} is the heat source generated by friction, thus:

$$q^{S^K} = \mu p_n V = \mu p_n \omega r$$

where: μ – friction coefficient, p_n – pressure on contact surface, ω – angular velocity, r – current radius of cylinder.

The temperature on the lateral surfaces of the elements S_b^C and S_b^M is also known. Heat from those surfaces is transferred to environment through heat exchange by convection according to the Newton equation. Thus, the fluxes can be expressed as follows:

$$q|_{S_b^M} = -\lambda_n^M T_{,n} = h_n(T^M - T^0),$$
$$q|_{S_b^C} = -\lambda_n^C T_{,n} = h_n(T^C - T^0) \tag{4}$$

where: $h_n \left[\frac{J}{m^2 s \circ K}\right]$ – surface film conductance by environment.

The problem of heat conduction in the process of friction welding determined by means of Eqs. (1–4) is, thus, reduced to calculation of temperature field, which is a function

of $T = T(x, y, z, t)|_{t=\text{const}}$. In the paper numerical solutions based of finite element method (FEM) are utilised [16].

In FEM it is postulated that the variational extremal principle is valid in all the calculation volumes $V^C + V^M$. For the modelled process of friction welding the principle corresponds to finding stationarity of the following functional:

$$
\begin{aligned}
\pi(T) = & \int\limits_{V^C+V^M} \frac{1}{2} k_i (T_{,i})^2 dV + \int\limits_{S^K} T\, q^{s^K} dS \\
& + \int\limits_{S_b^M+S_b^C} \frac{1}{2} h_n\, T^2 dS - \int\limits_{S_b^M+S_b^C} h_n T\, T^\circ dS.
\end{aligned}
\tag{5}
$$

It results from Eq. (5) that one has to determine the temperature field $T = T(x, y, z, t)|_{t=\text{const}}$ such that the functional $\pi(T)$ reach the minimum. Thus:

$$
\delta\pi\,(T) \equiv \frac{\partial \pi\,(T)}{\partial T} = 0.
\tag{6}
$$

3.1. Numerical determination of temperature field. The approximated variational solution (6) can be obtained by means of finite element method by introducing an interpolation function N, which approximates temperature distribution $T(x, y, z)$ in a single finite element on the basis of temperature values in characteristic nodes of the element T^e. For a single finite element approximation of temperature function $T(x, y, z)$ can be written:

$$
\begin{aligned}
T\,(x, y, z) &= \sum_{\alpha=1}^{A} N^\alpha\,(x, y, z)\, T^\alpha \\
&\equiv N^\alpha\,(x, y, z)\, T^\alpha
\end{aligned}
\tag{7}
$$

(in summation convention)

where: $N^\alpha(x, y, z)$ – interpolation function in an element (shape function), T^α – temperature value in the nodes of the element $\alpha = 1, 2, ..A$. Denoting $N^\alpha{}_{,n} = B^\alpha$ for derivative of the shape function the temperature gradient in Eq. (6) take the form:

$$
T_{,n} = B^\alpha T^\alpha.
\tag{8}
$$

The condition of minimisation $\delta\pi(T) = 0$ (with extending the integration from element on all considered volume) leads to fundamental dependence:

$$
K_{\alpha\alpha} T_\alpha - F_\alpha = 0
\tag{9}
$$

where:

$$
\begin{aligned}
K_{\alpha\alpha} = & \sum_e \int\limits_{V^e} B^{(e)T} k^{(e)} B^{(e)} dV \\
& + \sum_e \int\limits_{S_b^{M+C}} N^{(e)T} h N^{(e)} dS - \text{stiffness matrix}
\end{aligned}
\tag{10}
$$

$$
F_\alpha = -\sum_e \int\limits_{S^K} q^{S^K} N^{(e)} dS + \sum_e \int\limits_{S_b^{M+C}} N\, h\, T^0\, dS
\tag{11}
$$

– components of temperature load vector

the index T denotes transposition of matrix. Value T^α represents the searched temperature in the nodes in the solution of heat conduction problem in the process of inertia friction welding at gradual time increment. Solution of the equation system was obtained by means of FEM system – ADINA-T.

4. Mathematical modelling of thermo-mechanical effects

Mathematical modelling of thermo-mechanical effects was simplified by assumption that for the given time increment thermal and mechanical deformations are treated as quasi-stationary ones and the fields corresponding to these deformations are coupled. Thus, in the modelling of the welding process the field temperature (obtained from the heat problem solution) and mechanical load (the given pressure p_i on the end face of the ceramic workpiece) are considered.

Assuming that for the given time increment Δt the welded element is in the equilibrium state the problem can be described by means of the following system of equations in the incremental formulation:

$$
\Delta\sigma_{ij,j} = 0 \ - \text{equations of equilibrium without mass forces}
\tag{12}
$$

$$
\Delta\varepsilon_{ij} - \alpha\delta_{ij}\Delta T = {}^1\!/_2 (\Delta u_{i,j} + \Delta u_{j,i}) - \text{geometrical relations}
\tag{13}
$$

where: α – coefficient of thermal expansion, δ_{ij} – Kronecker symbol.

In the process of welding the ceramics undergoes elastic strains and the aluminium in certain areas is deformed plastically. Total strain rate $d\varepsilon$ can be defined as follows:

$$
d\varepsilon = d\varepsilon^e + d\varepsilon^p + d\varepsilon^T
\tag{14}
$$

where the constitutive equations for elastic, plastic and thermal strains have the form:

$$
d\varepsilon_{ij}^e = C_{ijkl}^e d\sigma_{kl}
\tag{15}
$$

$$
d\varepsilon_{ij}^e + d\varepsilon_{ij}^p = d\varepsilon_{ij}^{ep} = C_{ijkl}^{ep} d\sigma_{kl} = \left[C_{ijkl}^e - C_{ijkl}^p \right] d\sigma_{kl}
\tag{16}
$$

where: C_{ijkl}^e – elastic material compliance tensor; $C_{ijkl}^p = \frac{9 S_{ij} S_{kl}}{4\sigma_i^2 H}$ – tensor function of plastic material compliance; $\sigma_i = \sqrt{\frac{3}{2} S_{ij} S_{ij}}$; S_{ij}, S_{kl} – stress deviator; $H = \frac{d\sigma}{d\varepsilon^p}$ – modulus of plasticity for linear strain hardening;

$$
d\varepsilon_{ij}^T = -\alpha\delta_{ij} dT.
\tag{17}
$$

Inversion of Eqs. (14) and including (15), (16), (17) leads to Eq. (18)

$$
d\sigma_{ij} = \left[D_{ijkl}^e - \chi D_{ijkl}^p \right] d\varepsilon_{kl} - \beta_{ij} dT
\tag{18}
$$

D_{ijkl}^p – tensor function of plastic material properties [17],

$$
D_{ijkl}^p = 2G \left(\frac{S_{ij} S_{kl}}{S} \right); \quad S = \frac{2}{3}\sigma_i^2 \left(1 + \frac{H}{3G} \right)
$$

$\chi = 0$ when $\sigma_i < \sigma_{pl}$, $\chi = 1$ when $\sigma_i \geqslant \sigma_{pl}$; $\beta_{ij} dT$ – term of thermal stresses.

Boundary conditions for this problem:

$$p_i = \overline{p_i}\big|_{S^C} \quad \text{given load} \tag{19}$$

$$u_i = \overline{u_i} = 0\big|_{S^M} \quad \text{fixation condition} \tag{20}$$

$$u_i^C = u_i^M \big|_{S^K} \quad \text{displacement continuity condition} \tag{21}$$

$$\sigma_{ij}n_i = 0 \big|_{S_b^{M+C}} \quad \text{free surface condition.} \tag{22}$$

Variational formulation of this problem in displacement field (in the form of finite increments) can be defined on the basis of potential energy functional of the system:

$$\pi(\Delta u_i) = 1/2 \int_V \left[D_{ijkl}^{e-p}\Delta\varepsilon_{kl} - \beta_{ij}\Delta T \right] \\ \times \left[\Delta\varepsilon_{ij} - \alpha\delta_{ij}\Delta T \right] dV - \int_{S^C} \Delta p_i \Delta u_i \, dS \tag{23}$$

first term – strain internal energy in the volume $V = V^C + V^M$, second term – work of surface force on surface S^C.

The displacement field such that functional (23) reach the minimum has to be calculated.

$$\delta\pi(\Delta u) \equiv \frac{\partial\pi(\Delta u)}{\partial\Delta u} = 0. \tag{24}$$

4.1. Numerical determination of displacement field. Rough solution of the problem can be obtained using finite element method [16] and the following relation:

$$\Delta u(x,y,z) = \sum_{\gamma=1}^{A} N^\gamma(x,y,z)\Delta u^\gamma \equiv N^\gamma(x,y,z)\Delta u^\gamma \tag{25}$$

where: $N^\gamma(x,y,z)$ – interpolation function (shape function) in an element, Δu^γ – displacement values in the nodes of the finite element $\gamma = 1,2..A$.

Denoting the strain matrices, which result from differentiation of shape function matrices, as B_{ij}^γ:

$$\Delta\varepsilon_{ij} - \alpha\delta_{ij}\Delta T = N_{i,j}^\gamma\Delta u^\gamma = B_{ij}^\gamma\Delta u^\gamma \tag{26}$$

functional (23) in the discrete formulation takes the form:

$$\pi(\Delta u_\gamma) = \frac{1}{2}\int_V \left[D_{ijkl}^{e-p}\left(B_{kl}^\gamma\Delta u^\gamma + \alpha_{kl}\Delta T\right) - \beta_{ij}\Delta T \right] \\ \times B_{ij}^\gamma\Delta u^\gamma dV - \int_{S^C} \Delta p_i N_i^\gamma\Delta u^\gamma dS. \tag{27}$$

The condition of minimisation $\delta\pi(\Delta u) = 0$ leads to (integration in all the elements)

$$K_{\gamma\gamma}\Delta u^\gamma - \Delta P_\gamma = 0 \tag{28}$$

where:

$$K_{\gamma\gamma} = \sum_e \int_V D_{ijkl}^{e-p}B_{ij}^\gamma B_{kl}^\gamma dV - \text{stiffness matrix} \tag{29}$$

$$\Delta P_\gamma = \sum_e \int_V D_{ijkl}^{e-p}B_{ij}^\gamma \alpha_{kl}\Delta T dV \\ - \sum_e \int_V \beta_{ij}B_{ij}^\gamma\Delta T dV - \sum_e \int_{S^C}\Delta p_i N_i^\gamma dS \tag{30}$$

ΔP_γ – increment of force vector in nodes induced by the temperature field $\Delta T, \alpha, \beta$ and the load p_i acting on surface S^C.

The system of Eqs. (28) is an algebraic non-linear in respect of u^γ system that constitutes description of displacement model. Non-linearity is due to the non-linear function of elastic and plastic material properties.

5. Description of calculation model

In the calculation the conditions of the technological process were taken into account. The problem was considered as axisymmetric one and the calculation were carried out in cylindrical system. The process progressed in three stages:

1) heating with changeable with time heat flux,
2) forging under pressure increase,
3) cooling down and unloading after temperature equalisation.

Change of temperature field is generated by heat flux that depends on: pressure on the contact surface, relative velocity of the two faces and coefficient of friction. The pressure distribution is, in turn, a result of thermal deformation and local coefficient of friction is dependent on temperature. This mutual coupling requires many restarts of numerical calculations. In the calculations two FEM systems were utilised: ADINA, in which deformations and pressure distribution on contact surface were calculated, and ADINA-T, in which temperature field that depends on heat flux, conductivity and convection was determined. In Fig. 4 a graphical representation of the calculation model is shown. The following surfaces were denoted: contact surface, heat exchange surface and external loading surface. Due to the fact that aluminium heats up during the process to melting point thermal-elastic-plastic material was simulated. The material is characterised by the hardening curves, which depend on temperature, shown in Fig. 5 [18]. The ceramics was simulated as an elastic material. Melting point of the ceramics is 2220°C and modulus of elasticity 300 GPa. Coefficient of friction μ depends only on temperature. Change of μ with temperature is illustrated in Fig. 6.

Calculation cycle between the consecutive restarts is presented in Fig. 7. In the first numerical iteration the external load generates uniform pressure on the contact surface and consequently linearly changing heat flux. In the next iteration the pressure distribution on contact surface was calculated in ADINA. On the basis of the calculated pressure distribution heat flux was determined. The heat flux was then read in ADINA-T. The program was restarted and the calculated temperature field was read in to ADINA. After restart the calculation cycle was repeated. After heating up the area near the contact surface to the proper temperature the heat flux was equalled to zero and the external load was increased to 46 MPa.
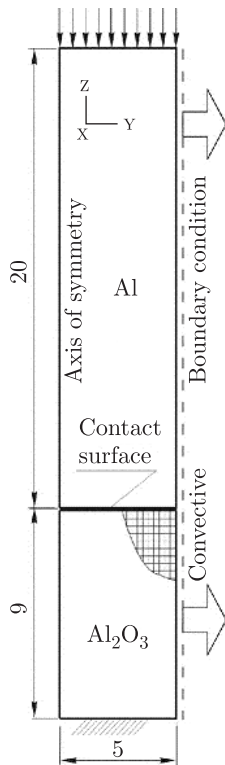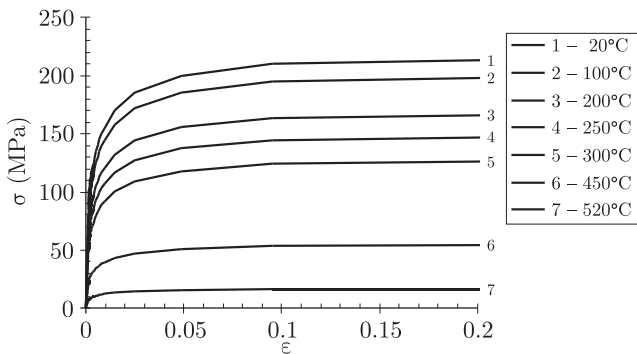
Fig. 4. FEM model

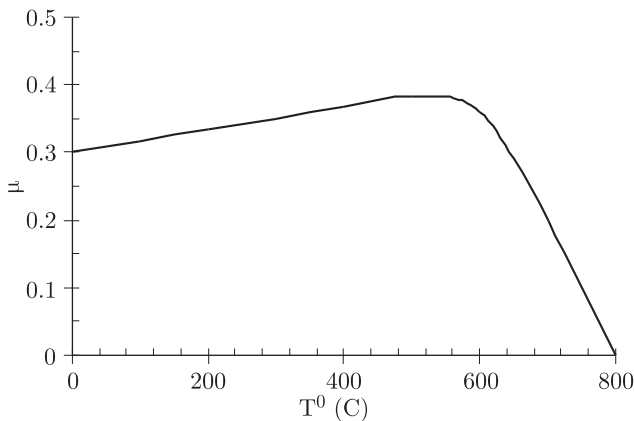Fig. 5. Hardening curves (Al) for different temperatures (after Ref. 18)

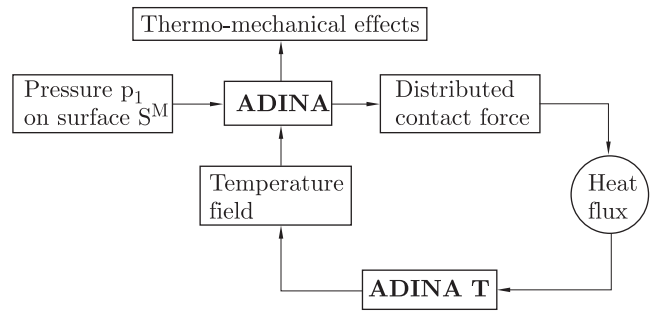Fig. 6. Friction coefficient versus temperature

Fig. 7. Flow chart of calculation of thermo-mechanical effects

Equalisation of temperature and unloading are the final stage of the calculations. In this stage the contact has to be replaced with proper boundary condition that simulates the process of element welding. If we perform calculations with contact during cooling down an interstice is forming on the contact surface near the symmetrical axis. By the size of the interstice one can assess the magnitude of residual stresses decreasing strength of the bond. The residual stresses arise during the stage of cooling down and are due to the fact that the thermal properties of the ceramics and aluminium are different

$$\left(\lambda^C = 16.7 \left[\frac{J}{smK}\right], \quad \lambda^{Al} = 170 \left[\frac{J}{smK}\right],\right.$$

$$\left.\alpha^C = 6.5 \cdot 10^{-6} \left[\frac{1}{K}\right], \quad \alpha^{Al} = 24 \cdot 10^{-6} \left[\frac{1}{K}\right]\right).$$

In Figs. 8 and 9 pressure distributions for selected solution times are shown. Non-uniform pressure distributions during the friction stage result from local thermal and plastic deformations of the aluminium. The deformations move towards the symmetrical axis of the workpieces and cause that the end faces of the elements are not in contact on the whole contact surface. Only in the final friction stage (t = 0.85 s), when the temperature is equalising in the welding area, the pressure distribution is more uniform. In Figs. 10 and 11 change of heat flux for the same solution times are presented. The heat flux depends on pressure distribution, thus, the changes are highly non-uniform. Temperature distributions on the contact surface are shown in Figs. 12 and 13.

In Fig. 14 temperature distribution on the lateral surfaces of the welded elements after 0.45 s of heating up is presented. The calculated temperature distribution is denoted with line and temperatures distribution measured with thermovision camera is shown by means of points. The coordination z = 0 corresponds to contact surface of both elements. Temperature distribution in the final stage is presented in Fig. 15. The maximal value of temperature is located in half of the workpiece radius. Such a temperature distribution is confirmed by metal science analysis [9]. The shape of the welded elements obtained from numerical calculations was compared to the profile obtained in the experiment (Fig. 16).
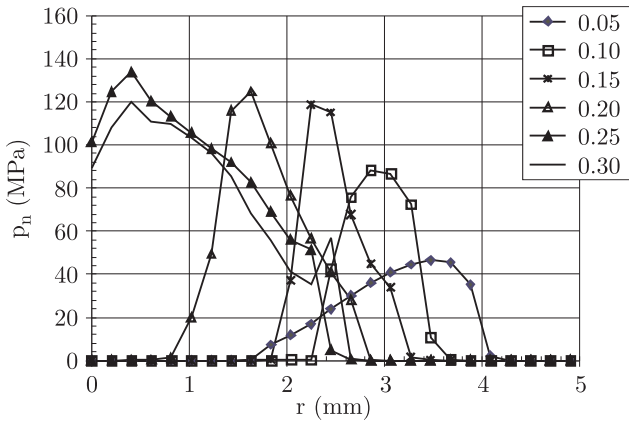
Fig. 8. Pressure distribution on contact surface in selected solution times
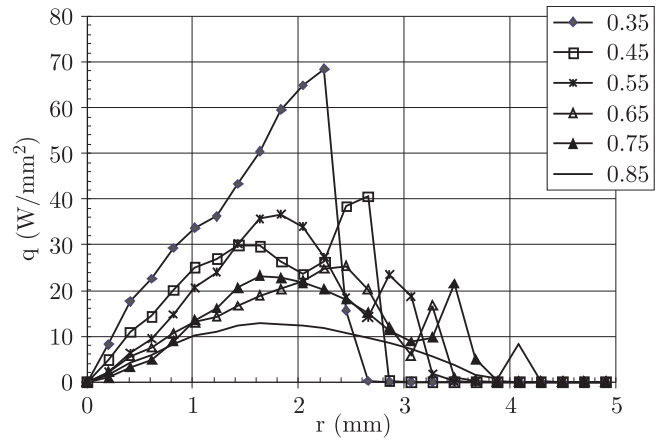

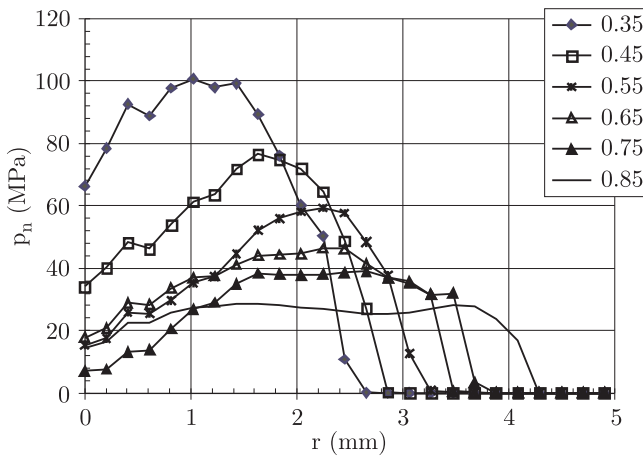Fig. 11. Heat flux distribution on contact surface in selected solution times

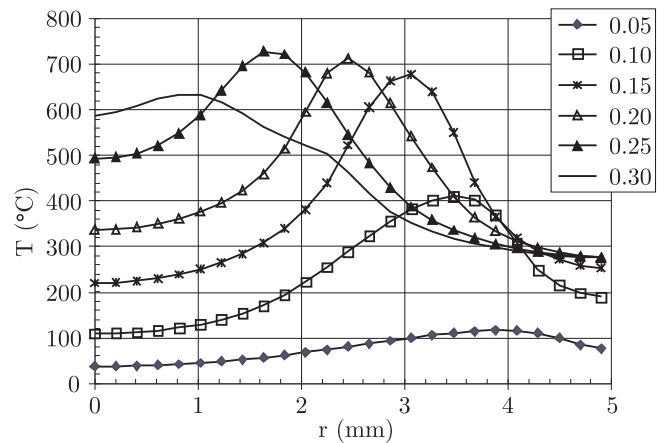Fig. 9. Pressure distribution on contact surface in selected solution times

Fig. 12. Temperature distribution on contact surface in selected solution times
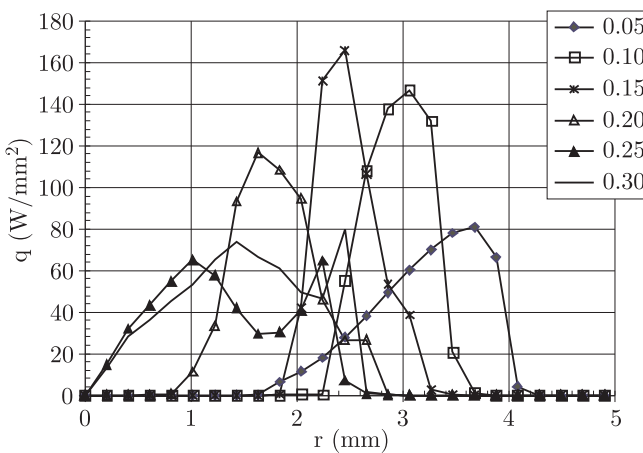

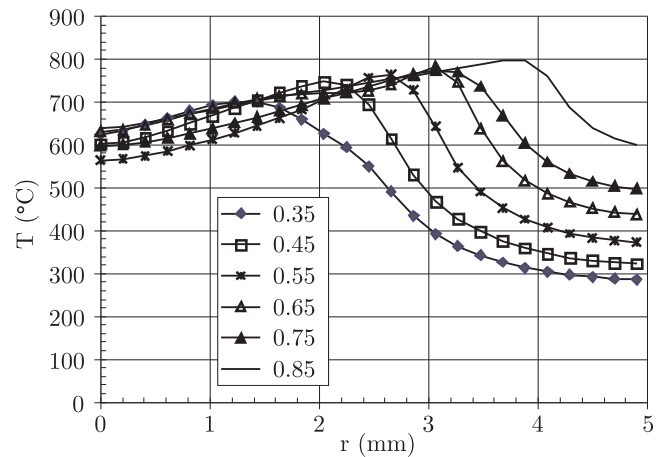Fig. 10. Heat flux distribution on contact surface in selected solution times

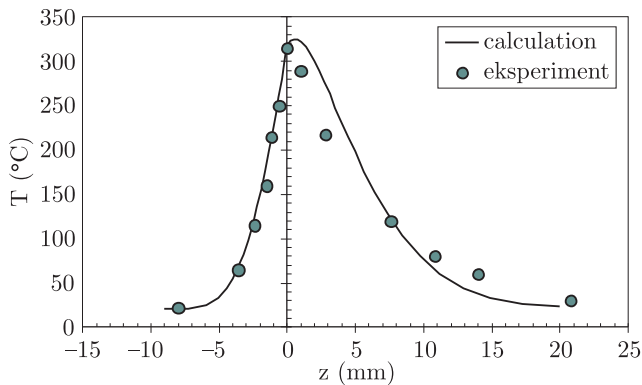Fig. 13. Temperature distribution on contact surface in selected solution times

Thermo-mechanical phenomena in the process of friction welding of corundum ceramics and aluminium

Fig. 14. Temperature distribution on lateral surface for time 0.45 s
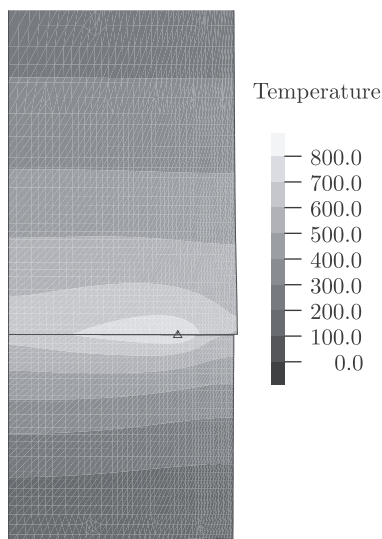(points – measured distribution)
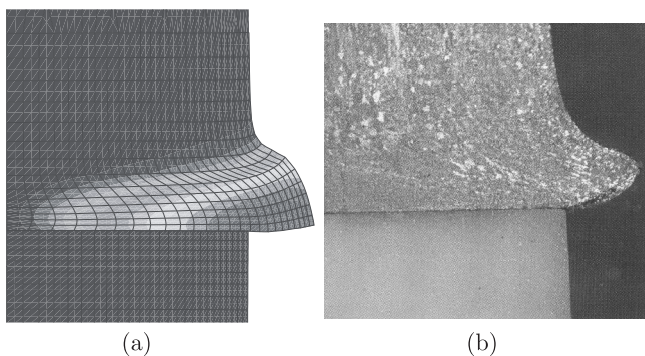

Fig. 15. Band of temperature after heating up

Fig. 16. Theoretical (a) experimental (after Ref.2); b) final rods profiles of Al_2O_3 and Al

6. Conclusions

1. Pressure distribution on the contact surface during friction heating-up is highly non-uniform, changes significantly especially in the initial stage of the process and is completely different from uniform linear distribution.

2. Calculations performed assuming coefficient of friction constant in a wide range of temperature indicate that such an assumption makes the changes of pressure and heat flux more uniform.

3. In the final stage of the process the temperature distribution on the contact surface is almost uniform, though the temperature in the external areas of the workpieces is lower during the whole time of heating-up process. The maximal value of temperature is located in half of the workpiece radius.

4. The strain analysis indicates that the circumferential areas of the workpiece surfaces of friction are in contact for the shortest time. This negatively influences the quality of bond in the areas (strength test of welds confirm this conclusion).

5. The results of numerical calculations are similar to temperature values measured on the external areas during the welding process, and the shapes of final profiles are also similar.

6. Relationship between coefficient of friction and temperature has to be studied for the welded materials.

7. In order to explain in a more detailed manner the phenomena that take place during welding of ceramics and metal the diffusion effects have to be also taken into consideration.

REFERENCES

[1] W. Włosiński, *The Joining of Advanced Materials*, Oficyna Wydawnicza PW, Warszawa, 1999.

[2] W. Włosiński and T. Chmielewski, "Conditions of friction welding and the structure of Al_2O_3-Al and Al_2O_3-Cu joints", *Welding Review* 12, 1–15 (2003), (in Polish).

[3] Ch. Dawers, "Joining of ceramics by friction heating and forging", *TWI*, www.twi.co.uk, (2001).

[4] S. Jones, "Can ceramics be friction welded to metals ?", *TWI*, www.twi.co.uk, (2003).

[5] A. Francis and R. Crane, *Int. J. Heat Transfer* 28, 1747 (1985).

[6] A. Rakhimov, Z. Li, and T. North, "Theoretical modeling of MMC base material friction joining", *Canadian Metallurgical Quarterly* 35 (3), 285–289 (1996).

[7] C.J. Cheng, "Transient temperature distribution during friction welding of two similar materials in tubular form", *Weld. Journal* 41 (12), 223–240 (1963).

[8] K. Wang and P. Naggapan, "Transient temperature distribution in inertial welding of steels", *Weld. Journal* 49 (7), 419–426 (1970).

[9] A.Z. Sahin, B.S. Yibas, M. Ahmed, and J. Nickel "Analysis of the friction welding process", *Journal of Materials Processing Technology* 82, 127–136 (1998).

[10] A. Ambroziak, *Welding of Infusible Metals in Liquid Against a Background of Other methods of Bonding*, Publishing House of Wrocław University of Technology, Wrocław, 1998, (in Polish).

[11] L.D. Alvise, E. Massoni, and S.J. Walloe, "Finite element modeling of the inertia friction welding process between dissimilar materials", *J. Mat. Processing Technology* 125–126, 387–391 (2002).

[12] L. Fu, L. Duan, "The coupled deformation and heat flow analysis by finite element method during friction welding", *Weld. J.* 77 (5), 202–207 (1998).

[13] M. Kleiber and A. Służalec, "Finite element analysis of heat flow In friction welding", *Rozp. Inż.* 32 (1), 107–113 (1984).

[14] A. Służalec, "Thermal effects in friction welding", *Int. J. Mech. Sci.* 32 (6), 467–478 (1990).

[15] A. Służalec, "Solution of thermal problems in friction welding", *Int. J. Heat Mass Transfer* 36, 1583–1587 (1993).

[16] K.J. Bathe, *Finite Element Procedures*, New Jersey, 1996.

[17] Y. Yamada, "Plastic stress-strain matrix and its application for the solution of elastic-plastic problems by the finite element method", *Int. J. Mech. Sci.* 10, 343 (1968).

[18] M. Perzyk, "Validity of constitutive equations used for calculation of stresses in cooling castings", *Materials Science and Technology* 1, 84–92 (1985).